Effect of Fe and Si on the microstructure and phase composition of the aluminium-calcium eutectic alloys

UDC 669.71.055

N. A. Belov, *Professor of the Department of Metal Forming*[1]
T. K. Akopyan, *Research Fellow*[1,2], *e-mail: aktorgom@gmail.com*
S. S. Mishurov, *Leading Engineer*[1]
N. O. Korotkova, *Post-Graduate Student of the Department of Metal Forming*[1]

[1] *National University of Science and Technology MISiS, Moscow, Russia.*
[2] *Baikov Institute of Metallurgy and Materials Science, Moscow, Russia.*

Using both thermodynamic calculations and experimental analises, the Al – Ca – Fe – Si phase diagram near the aluminum corner has been studied. It is shown that the Al_4Ca intermetallic phase can be in equilibrium with the Al_3Fe and Al_2CaSi_2 phases, which are included in the invariant eutectic reaction $L \rightarrow$ (Al) + Al_4Ca + Al_2CaSi_2 + Al_3Fe at 611 °C, 91.90% Al, 6.92% Ca, 0.68% Fe, and 0.50% Si. In accordance with the literary data and results of the experiments, the binary Al_3Fe iron-containing phase can be replaced by a ternary $Al_{10}CaFe_2$ phase. The solidification of all Al – Ca alloys should be completed via this invariant reaction. A study of the hypoeutectic alloys with calcium content up to 6 % (wt.), iron to 1% (wt.) and silicon to 1% (wt.), revealed a fine microstructure consisting of primary crystals of (Al) and eutectic colonies. Fe- and Si-bearing phases have favourable morphology. Coarse needle-like particles were not found. In accordance with the results of DSC analysis and calculation data, the solidification range of the considered alloys is very narrow and less than 50 degrees, which suggests excellent casting properties. In particular, according to the casting "pencil" and "harp" probes for the Al6Ca1Fe0.5Si alloy with minimal solidification range, it is not inferior to standard Al – Si alloys. Due to the results above, it can be conclude that the Al – Ca system is promising for the development of new casting aluminium alloys.

Key words: Al – Zr – Sc alloys, $Al_3(Zr, Sc)$ nanoparticles, electrical resistance, strength, annealing.
DOI: *10.17580/nfm.2017.02.07*

Introduction

The Al – Ca system is promising for the development of a new generation of cast aluminium alloys [1]. Calcium, as well as silicon, forms a eutectic-type diagram with aluminium. The concentration of calcium in the binary eutectic is about 7.6% (wt.) and the corresponding temperature is about 617 °C [2–4]. The distinguishing feature of this eutectic is that the fraction of the second Al_4Ca phase exceeds 30% (vol.), which is three times that in the Al – Si eutectic. This allows us to achieve a combination of various properties in the Al – Ca alloys (they may be called by "eutectic composites"). In particular, it was found in Ref. [5] that alloys based on the binary (Al) + Al_4Ca eutectic have high castability compared with commercial Al – Si alloys.

It is known that the presence of iron and silicon, as well as harmful impurities, is inevitable in most aluminium alloys (when they are not alloying elements) [6, 7]. The mechanical properties of castings (especially ductility) are largely dependent on the morphology of the Fe- and Si-containing phases [8–10]. So the Al – Ca – Fe – Si system should be considered because it allows studying the combined effect of iron and silicon on the phase composition and structure of Al – Ca alloys. According to the available information [2, 11–13], in the alloys of the Al – Ca – Fe – Si system, the following phases, Al_4Ca, Al_3Fe, (Si), Al_5FeSi, Al_8Fe_2Si and Al_2CaSi_2, may be in equilibrium with (Al). In addition to these known phases, iron and calcium form a ternary compound with aluminium, whose composition corresponds to the formula $Al_{10}CaFe_2$ [14]. Thus, the expected structure of the Al – Ca – Fe – Si system in the aluminium corner is rather complicated.

Based on the above and taking into account the scarcity of information on the considered quaternary system, the main task of this work is identified as the study the effect of Fe and Si on the microstructure and phase composition of the aluminium–calcium eutectic alloys.

Phase composition of Al – Ca – Fe – Si system

Quantitative analysis of the phase composition of the quaternary system under consideration was carried out using Thermo-Calc software [15]. Since there is no ternary

$Al_{10}CaFe_2$ compound in the thermodynamic database (TTAL5), the results of the calculations were critically evaluated by taking into account this incompleteness.

The calculation of isothermal section of considered quaternary system at 90% Al (Fig. 1, *a*) allows to reveal the equilibrium between various phases in aluminium corner. According to calculation the Al_4Ca compound may be in equilibrium with phases Al_3Fe and Al_2CaSi_2. All these phases participate in invariant eutectic reaction $L \rightarrow (Al) + Al_4Ca + Al_2CaSi_2 + Al_3Fe$ at 611 °C, 91.90% Al, 6.92% Ca, 0.68% Fe, and 0.50% Si. Based on results reported in [14] we have added the compound $Al_{10}CaFe_2$ in this calculated section. If we assume equilibrium between the ternary compounds Al_2CaSi_2 and $Al_{10}CaFe_2$ (dotted line in Fig. 1, *a*), we should expect the invariant eutectic reaction $L \rightarrow (Al) + Al_4Ca + + Al_2CaSi_2 + + Al_{10}CaFe_2$. It is expected that the desired structure can be obtained for alloys near this quaternary eutectic.

The liquidus projections of Al – Ca – Fe – Si system were calculated also. As can be seen from Fig. 1, *b*, in the section at 6% Ca the primary crystals of the compounds are not formed with the introduction of both iron and silicon at the same contents as in the ternary systems. This result is favourable, since it assumes a sufficiently large allowable total concentration of these elements. Moreover, if we take into account the expansion of the primary crystallisation region of the (Al) in the case of accelerated solidification (casting in metal moulds), we can expect larger allowable concentrations of Fe and Si (see the dotted line in Fig. 1, *b*). The section calculated at 10% Ca shows three fields of primary solidification of Ca-containing compounds (Fig. 2, *c*).

The reactions that occur during solidification can be traced using the vertical sections shown in Fig. 2. Based on the presence of $Al_{10}CaFe_2$ in the Al – Ca alloys, the Al_3Fe phase (which gives the calculation) has been replaced by this ternary compound. The horizontal line at the cross sections corresponds to the invariant eutectic reaction $L \rightarrow (Al) + Al_4Ca + Al_2CaSi_2 + Al_{10}CaFe_2$ at 611 °C (see Fig. 2). The solidification of all Al – Ca alloys should be completed via this reaction. In addition to the primary crystals ((Al) or ternary compounds) and quaternary eutectics, the formation of binary and ternary eutectics with an aluminium solid solution and the Al_4Ca, Al_2CaSi_2 and $Al_{10}CaFe_2$ phases (depending on the Fe and Si contents) should also be expected in these alloys. For example, in the alloy with 6% Ca, 0.5% Fe and 0.5% Si (marked in Fig. 2, *a*), the following sequence of reactions should take place under equilibrium conditions: $L \rightarrow (Al)$; $L \rightarrow (Al) + Al_2CaSi_2$; $L \rightarrow (Al) + Al_2CaSi_2 + Al_4Ca$; $L \rightarrow (Al) + Al_4Ca + Al_2CaSi_2 + Al_{10}CaFe_2$. In alloys with ratio Fe:Si far from 1:1 the ternary compounds (Al_2CaSi_2 or $Al_{10}CaFe_2$) should form at the beginning of solidification. With a decrease in the calcium content, the region of the (Al) primary crystallisation in quaternary system is expanded (it means that total sum of iron and

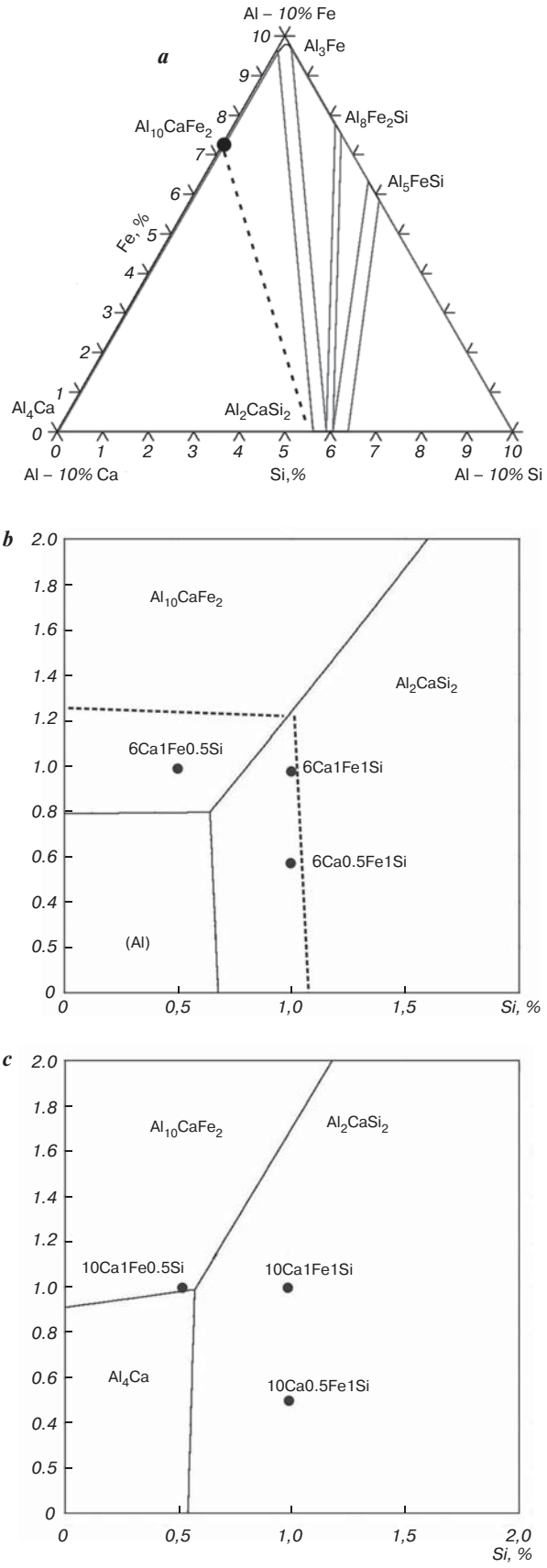

Fig. 1. Calculated isothermal section (*a*) and liquidus projections (*b*, *c*) of the Al – Ca – Fe – Si system in the aluminium corner: *a* — at 90% Al and 575 °C; *b* — at 6 %Ca; *c* — at 10% Ca

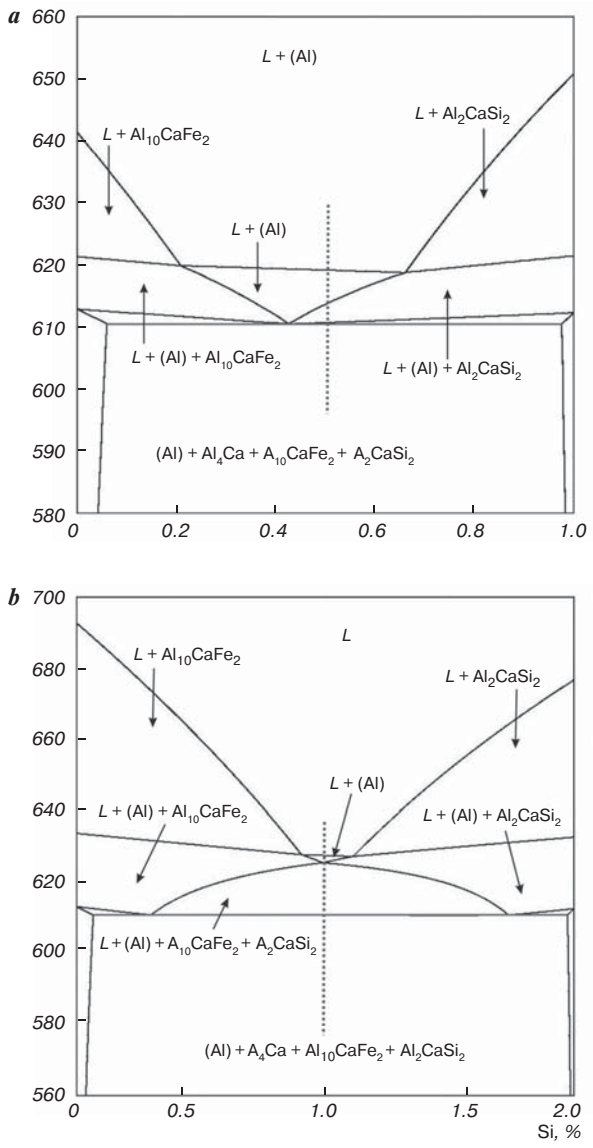

Fig. 2. Calculated vertical sections of the Al – Ca – Fe – Si system in the aluminium corner:
a — vertical section at 93% Al and 6% Ca (Fe + Si = 1%);
b — vertical section at 94% Al and 4% Ca (Fe + Si = 2%)

silicon may be higher). For example, the alloy with 4% Ca, 1% Fe and 1% Si (marked in Fig. 2, *b*) should be free from primary crystals of ternary aluminides (Fig. 2, *b*).

Material and methods

The experimental study was focused on nine quaternary alloys of the Al – Ca – Fe – Si system containing 4, 6 and 10% Ca (hypoeutectic, near-eutectic and hypereutectic, correspondingly). The nominal compositions of these alloys (given in Table 1) were sufficiently close to the actual. Melting was carried out in an electric resistance furnace in a graphite-chamotte crucible based on high purity aluminium (99.99%). Calcium and iron were introduced into an aluminium melt in the form of binary

Table 1

Chemical composition of experimental alloys and calculated parameters of solidification

Designation of alloy	Concentration, % (wt.)			Parameters of solidification[1]			
	Ca	Fe	Si	T_L, °C	T_S, °C	ΔT, °C	Q_E, %
4Ca1Fe0.5Si	4	1	0.5	631	611	20	52
4Ca0.5Fe1Si	4	0.5	1	630	611	19	47
4Ca1Fe1Si	4	1	1	627	611	16	47
6Ca1Fe0.5Si	6	1	0.5	637	611	26	84
6Ca0.5Fe1Si	6	0.5	1	651	611	40	74
6Ca1Fe1Si	6	1	1	651	611	40	78
10Ca1Fe0.5Si	10	1	0.5	660	611	49	84
10Ca0.5Fe1Si	10	0.5	1	704	611	93	74
10Ca1Fe1Si	10	1	1	704	611	93	84

[1] T_L —liquidus temperature; T_S — soliidus temperature; ΔT ($T_L - T_S$) — solidification interval, °C; Q_E —mass fraction of quaternary eutectic.

master alloys (Al – 15% Ca and Al – 10% Fe, respectively), while silicon was in pure form. The melt was poured into a graphite mould at a temperature of ~750 °C to obtain flat ingots with dimensions of 15×30×180 mm (the cooling rate during solidification was ~10 K/s). Samples were extracted from the obtained castings to study the structure and properties. Estimation of the casting properties of experimental alloys was carried out using various probes for fluidity and hot tearing [11], as well as by producing shaped castings into metal moulds. Heat treatment of the samples was carried out in SNOL muffle electric furnaces.

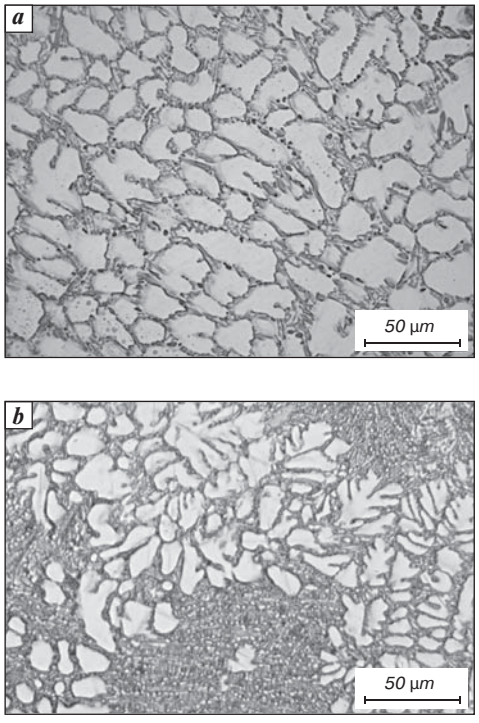

Fig. 3. Microstructures of hypoeutectic alloy 4Ca1Fe0.5Si (*a*) and near eutectic alloy 6Ca1Fe1Si (*b*), OM

The structure was examined using optical microscopy (OM, Axiovert 200 MMAT) and scanning electron microscopy (SEM, TESCAN VEGA 3) equipped with an electron microprobe analyser (EMPA, Oxford Instruments, Aztec software). Polished samples cut from the central part of the ingots and sheets were studied. Mechanical polishing (Struers Labopol-5) was used, as well as electrolytic polishing, as these methods are complementary and enable complete observation of the microstructure. Electrolytic polishing was achieved using 12 V in an electrolyte containing six parts ethanol, one part $HClO_4$ and one part glycerine.

Differential scanning calorimetry with a heating and cooling rate of 10 K/min was performed using a high temperature DSC Setaram Setsys Evolution. The experiment was carried out in a dynamic Ar atmosphere with a flow rate of 50 ml/min. A temperature accuracy of ±0.5 °C was obtained.

Experimental results and discussion

The microstructure of the slow solidified alloy with 6% Ca, show some primary crystals of ternary compounds in agreement with the calculated liquidus surface (Fig. 2, *b*). Alternatively, in castings obtained in graphite form, there are no primary Ca-containing compounds. The main structural components in alloys with 4% Ca and 6% Ca are both primary crystals of (Al) and eutectic colonies (Fig. 3, *a*, *b*). The fraction of eutectic in alloys with 6% Ca, as expected, is higher. In all experimental alloys eutectic has a fine structure (Fig. 4, *a*). Calcium, iron and silicon are concentrated in the eutectic (Fig. 4, *b*–*d*). The contents of these elements in (Al) are negligible. A needle-like form of the primary intermetallic compounds is clearly identified in the alloys containing 10% Ca (Fig. 5, *a*). According to the EMPA results, they are enriched with calcium (Fig. 5, *b*).

The solidus of all experimental alloys is ~613 °C (Fig. 6), which is close to the results of the calculation (see in Table 1). According to the known empirical laws, the combination of a narrow solidification range and a high fraction of eutectic suggests excellent casting properties [11]. Experimental results confirm this suggestion. The alloy 6Ca1Fe0.5Si with minimal solidification range (see in Fig. 6) was selected for further consideration. In particular, according to the "pencil" and "harp" probes, this alloy is not inferior to standard Al – Si alloys. As an example, in Fig. 7 is shown shaped castings produced from the 6Ca1Fe0.5Si alloy.

The fine structure of the eutectic suggests the possibility of obtaining globular particles of intermetallic phases during annealing [11]. A finer structure provides a reduction in the annealing temperature at which the

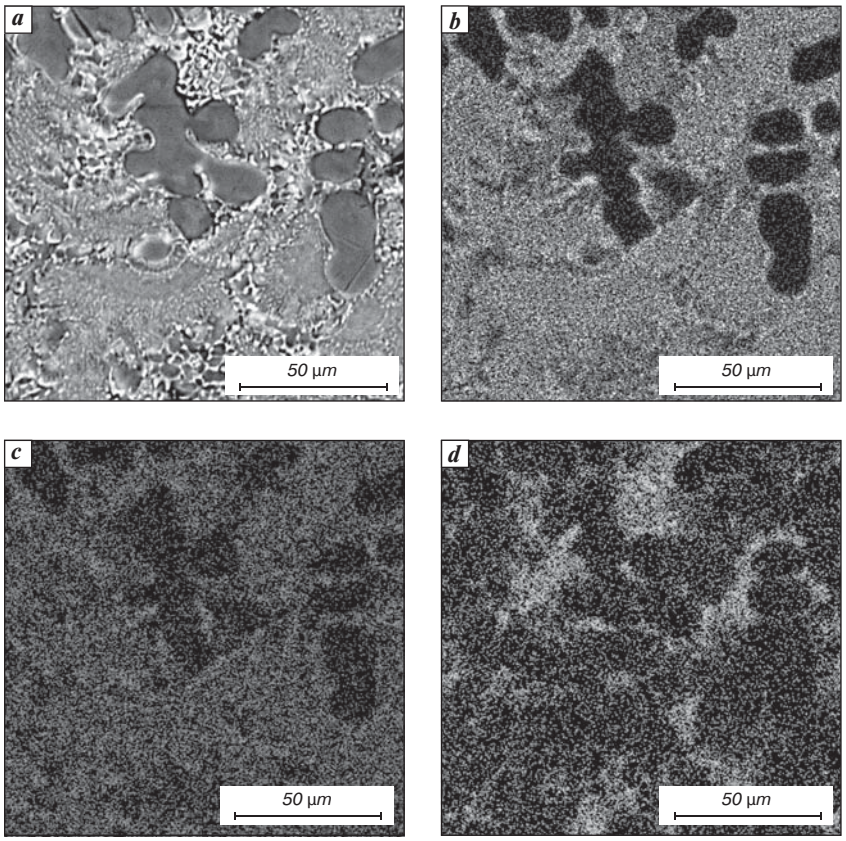

Fig. 4. SEM image (*a*) and EMPA elemental mapping of Ca (*b*), Fe (c), and Si (*d*) in the near-eutectic alloy 6Ca1Fe1Si

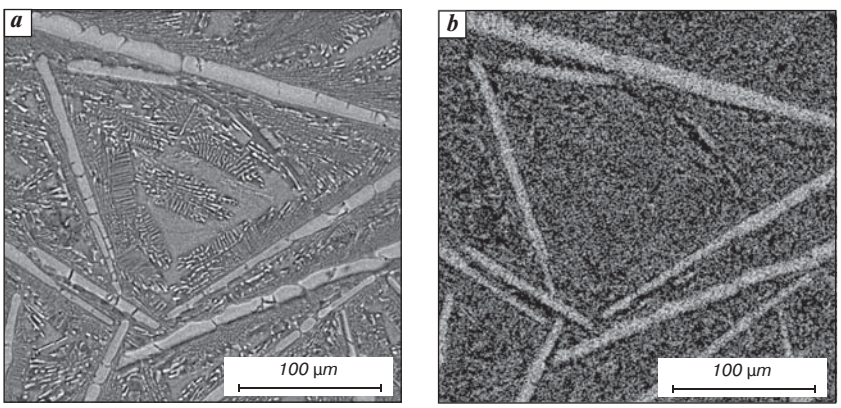

Fig. 5. SEM image (*a*) and EMPA elemental mapping of Ca (*b*) in the hipereutectic alloy 10Ca1Fe1Si

formation processes begin. The eutectic alloys of both binary systems (Al – Ni [16, 17] and Al – Ce [18]) and more complex ones (Al – Si – Ni [19] and Al – Mg – Si [20–22]) can be examples of this. The high solidus temperature of the experimental alloys (Table 1) allows inclusive annealing up to 600 °C. At this temperature, there is not only the spheroidisation, but also sufficiently strong coarsening, resulting in the formation of particles with a size of ~3 μm (Fig. 8). The microstructure after such annealing may be considered as equilibrium. The presence of three types of Ca-containing phases confirm the proposed variant of Al – Ca – Fe – Si phase diagram (see in Fig. 1, 2).

Tensile tests results (Table 2) of the flat samples (15 mm wide with four different thicknesses of 1.9, 2.8, 5.1 and 6.5 mm) obtained from a die casting machine show that the Al6Ca1Fe0.5Si alloy exhibits higher strength compared to the binary Al - Si A413 alloy (up to 1.3% Fe), which has the typical value of UTS about 160 MPa [11]. The high stability of the mechanical properties of the alloy Al6Ca1Fe should be noted. In particular, the scatter of UTS values does not exceed 10 MPa. Herewith, the influence of the sample thickness (h) on the mechanical properties is insignificant.

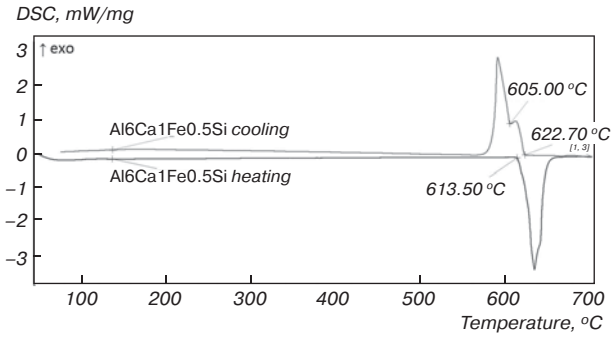

Fig. 6. DSC heating and cooling curves for the near eutectic alloy Al6Ca1Fe0.5Si

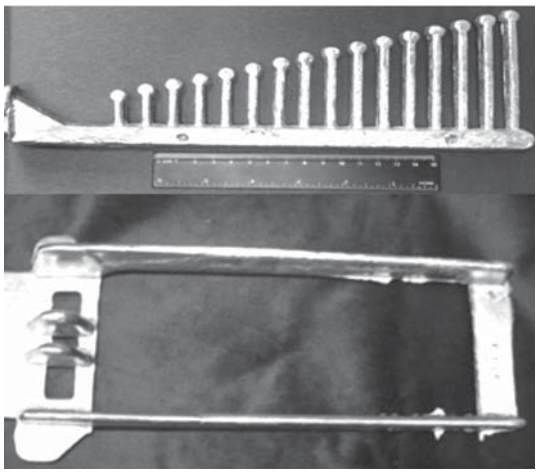

Fig. 7. Shaped castings from near eutectic alloy Al6Ca1Fe0.5Si

Table 2

Tensile properties of alloy Al6Ca1Fe0.5Si (die castings)

h^1, mm	*YS*, MPa	*UTS*, MPa	El, %
1.9	108±3	202±10	1.7±0.3
2.8	107±1	222±2	2.2±0.2
5.1	119±19	212±6	2.0±0.1
6.5	109±3	200±8	2.0±0.2

[1] Thickness of die casting sample.

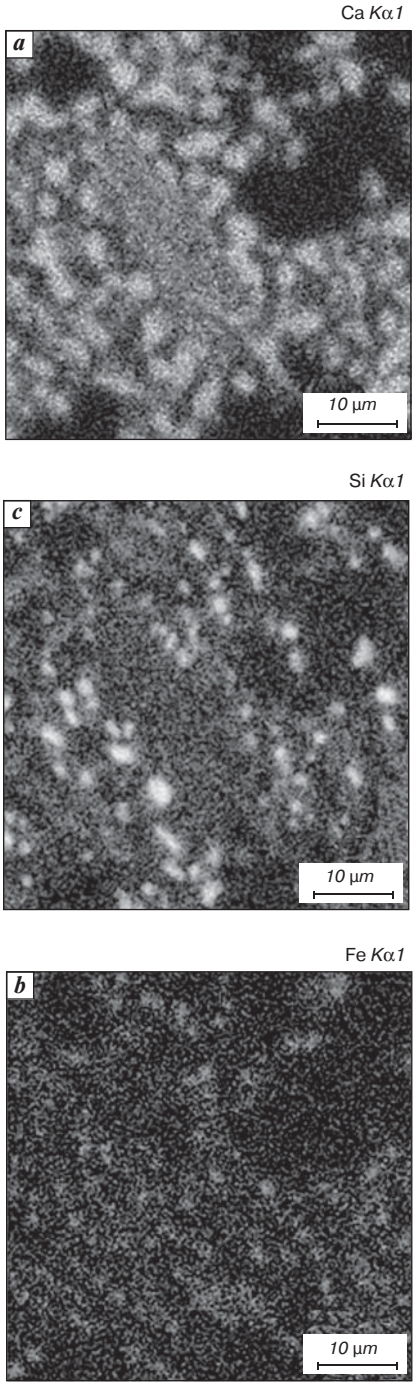

Fig. 8. EMPA elemental mapping of Ca (*a*), Fe (*b*), and Si (*c*) in the near-eutectic alloy Al6Ca1Fe0.6Si after annealing: at 600 °C (3 hours)

Due to the above mentioned results, it can be seen that the Al – Ca system is promising for the development of new casting aluminium alloys with structure, which is typical for the structure of aluminium matrix composites.

Conclusion

1. The phase composition of the Al – Ca – Fe – Si system in aluminium corner, including the phase equilibrium in the solid state and solidification reactions, has been calculated. The addition of iron and silicon to Al – Ca alloys leads to the appearance of the ternary compounds Al_2CaSi_2 and $Al_{10}CaFe_2$. These phases participate in the invariant eutectic reaction $L \rightarrow (Al) + Al_4Ca + Al_2CaSi_2 + Al_{10}CaFe_2$ at 611 °C.

2. It has been shown that alloys near the quaternary eutectic have the best structure, which is typical for the structure of aluminium matrix composites. Fe- and Si-bearing phases have favourable morphopogy. Coarse needle-like particles were not found.

3. Based on the experimental model near eutectic alloy containing 6% Ca, 1% Fe and 0.5% Si, it is shown that aluminium-calcium eutectic alloys are promising for the development of new casting aluminium alloys. This is due to the combination of a narrow temperature range of solidification and a favourable morphology of the eutectic.

This work was financially supported by the Ministry of Education and Science of the Russian Federation within the implementation of the Agreement on subsidies No. 14.578.21.0220 (unique identifier of the project RFMEFI57816X0220).

References

1. Belov N. A., Naumova E. A., Akopyan T. K. Eutectic alloys based on aluminum: new alloying systems. Moscow : "Ore and Metals" Publishing House, 2016. 256 p.

2. Mondolfo L. F. Aluminium alloys: structure and properties. Butterworths, London, 1976.

3. Kevorkov D., Schmid-Fetzer R. The Al – Ca system, part 1: experimental investigation of phase equilibria and crystal structures. *Z. Metallkd*. 2001. No. 92. pp. 946–952.

4. Ozturk K., Chen L. Q., Liu Z.-K. Thermodynamic assessment of the Al – Ca binary system using random solution and associate models. *Journal of Alloys and Compounds*. 2002. No. 340. pp. 199–206.

5. Belov N. A., Naumova E. A., Alabin A. N., Matveeva I. A. Effect of scandium on structure and hardening of Al – Ca eutectic alloys. *Journal of Alloys and Compounds*. 2015. No. 646. pp. 741–747.

6. Kaufman J. G., Rooy E. L. Aluminum alloy castings: properties, processes, and applications. ASM International. Ohio, 2004.

7. Hatch J. E. Aluminum: properties and physical metallurgy. ASM International. Ohio, 1984.

8. Ji S., Yang W., Gao F., Watson D., Fan Z. Effect of iron on the microstructure and mechanical property of Al – Mg – Si – Mn and Al – Mg – Si die cast alloys. *Materials Science & Engineering*. 2013. Vol. 564. pp. 130–139.

9. Moustafa M. A. Effect of iron content on the formation of β-Al_5FeSi and porosity in Al – Si eutectic alloys. J*ournal of materials processing technology*. 2009. No. 209. pp. 605–610.

10. Basak C. B., Hari Babu N. Morphological changes and segregation of β-$Al_9Fe_2Si_2$ phase: a perspective from better recyclability of cast Al – Si alloys. *Materials & Design*. 2016. No. 108. pp. 277–288.

11. Zolotorevskiy V. S., Belov N. A., Glazoff M. V. Casting aluminum alloys. Elsevier, Amsderdam, 2007.

12. Petzow G., Effenberg G. Ternary alloys: a comprehensive compendium of evaluated constitutional data and phase diagrams. Wiley-VCH; Weinheim, 1990. 647 p.

13. Belov N. A., Naumova E. A., Akopyan T. K. Effect of 0.3 wt%Sc on structure, phase composition and hardening of Al – Ca – Si eutectic alloys. *Transactions of Nonferrous Metals Society of China*. 2017. No. 4. pp. 741–746.

14. Belov N. A., Naumova E. A., Ilyukhin V. D., Doroshenko V. V. Structure and mechanical properties of Al – 6%Ca – 1%Fe alloy foundry goods, obtained by die casting. *Tsvetnye Metally*. 2017. Iss. 3. pp. 69–75.

15. Reference data for thermodynamic calculations. Available at: http://www.thermocalc.com. 2017 (accessed: 31.08.17).

16. Ratke L., Alkemper J. Ordering of the fibrous eutectic microstructure of Al-Al3Ni due to accelerated solidification conditions. *Acta Materialia*. 2000. Vol. 48. pp. 1939–1948.

17. Li X., Fautrelle Y., Ren Zh., Zhang Yu. , Esling C. Effect of a high magnetic field on the Al – Al_3Ni fiber eutectic during directional solidification. *Acta Materialia*. 2010. Vol. 58. pp. 2430–2441.

18. Plotkowski A., Rios O., Sridharan N., Sims Z., Unocic K., Ott R. T., Dehoff R. R., Babu S. S. Evaluation of an Al – Ce alloy for laser additive manufacturing. *Acta Materialia*. 2017. Vol. 126. pp. 507–519.

19. Böyük A., Engin S., Maraşlı N. Microstructural characterization of unidirectional solidified eutectic Al – Si – Ni alloy. *Materials Characterization*. 2011. Vol. 62. pp. 844–851.

20. Fatemi-Jahromi F., Emamy M. An investigation into high temperature tensile behavior of hot-extruded Al – 15wt%Mg_2Si composite with Cu – P addition. *Manufacturing Science and Technology*. 2015. Vol. 3. pp. 160–169.

21. Emamy M., Emami A. R., Tavighi K. The effect of Cu addition and solution heat treatment on the microstructure, hardness and tensile properties of Al–15%Mg2Si–0.15%Li composite. *Materials Science and Engineering:* A. 2013. Vol. 576. pp. 36–44.

22. Zhang J., Fan Z., Wang Y. Q., Zhou B. L. Microstructural development of Al–15 wt.% Mg_2Si in-situ composite with michmetal addition. *Materials Science and Engineering: A*. 2000. Vol. 281. pp. 104–112.

Analysis of the phase composition and microstructure of a TNM-type alloy by using thermodynamic calculation

UDC 669.71.055

T. K. Akopyan, *Research Fellow of the Department of Metal Forming*[1,2],
e-mail: nemiroffandtor@yandex.ru
N. O. Korotkova, *Post-Graduate Student of the Department of Metal Forming*[1]
A. P. Dolbachev, *Engineer of the Department of Metal Forming*[1]

[1] *National University of Science and Technology MISiS, Moscow, Russia.*
[2] *Baikov Institute of Metallurgy and Materials Science, Moscow, Russia.*

Using both thermodynamic calculations and experimental analyses, the phase composition and microstructure of the new TNM-type alloy with the following actual compositions, % (at.): TNM – 40.05 Al, 4.51 Nb and 1.05 Mo have been analysed. According to thermodynamic calculation, equilibrium solidification of the new alloy proceeded via the β-phase, i. e. $L \rightarrow L + \beta \rightarrow \beta$, followed by the solid-state transformations, the main of which is the eutectoid reaction $\alpha \rightarrow \alpha_2 + \beta + \gamma$. The microstructure of the alloy in the as-cast state and after high-temperature vacuum annealing was examined by means of scanning electron microscopy and electron microprobe analysis. Experimental studies have shown that the main structural component is the lamellar γ/α_2-colonies (with a thickness of individual plates of about 300 nm) surrounded by the β- and γ-phase crystals, the total fraction of which does not exceed 30% (vol.). According to the electron microprobe analysis, β-phase contains the largest amount of molybdenum, while the concentration of aluminium is the smallest. In contrast, the γ/α_2-colonies (initial α-phase) and γ-phase have higher aluminium and minimum molybdenum content. The observed results are in a good agreement with the results of the thermodynamic calculation. Experimental quantitative analysis of the phase fraction after vacuum annealing at 1250 °C of the new alloy has revealed that the total amount of β-phase does not exceed 8% (vol.), what practically corresponds to the base TNM (Ti43.5Al4Nb1Mo) alloy after similar heat treatment. However, the base alloy also contains up to 14% of the γ-phase, which is not observed in the new alloy. After annealing at 1100 °C, new alloy contains up to 24% (vol.) β-phase and 4% (vol.) γ-phase, while the base TNM alloy contains up to 14% (vol.) β-phase and 21% (vol.) γ-phase. In general, we can conclude that a reduction of aluminum content from 43.5 to 40.0% (at.) leads to a considerable increase in the amount of β-phase and decrease the γ-phase content. It is necessary to note, the calculated quantitative data of the phase fraction depending on the alloy annealing temperature are far from experimentally obtained data. However, a qualitative analysis of the change the phase relationship depending on the annealing temperature or chemical composition of the alloy, as well as the chemical composition of the phases is available.

Key words: titanium aluminides,γ-alloys, thermodynamic calculations, solidification, microstructure, phase composition, annealing.

DOI: *10.17580/nfm.2017.02.08*

Introduction

Titanium aluminide (TiAl) based alloys (hereafter referred to as γ-alloys) are considered as promising for manufacturing the blades of next generation gas turbine engines instead of nickel super-alloys [1–4]. These alloys should possess advanced technological properties [5–10] combined with appropriate strength, ductility, fatigue resistance and, most importantly, high temperature strength [4, 11, 12]. In order to achieve the required technological and mechanical properties (at room and elevated temperatures), the so-called 3rd generation γ-alloys such as the TNM alloy (with a nominal composition of Ti43.5Al4Nb1Mo0.1B (in % (at.))) [13–15] have been developed. This class of alloys has compositions that stabilize the β-phase so that this is the first phase to precipitate on solidification and is the only phase present immediately after solidification is complete (so called β-solidifying alloys) [16]. The fine as-cast microstructure, oxidation resistance and hot workability of these types of alloys have led to significant interest [17–19].

The phase composition of the γ-alloys is characterized by a high sensitivity to small changes in the concentration of alloying elements and heat treatment parameters [20–23]. Since the phase composition determines the structure of the alloys and, ultimately, their properties, its control is required for providing the specified operating characteristics. To analyse the phase composition of the TNM alloys we need to consider a phase diagram of at least four-components: Ti, Al, Nb and Mo. This had been partially studied in [1, 22, 24]. Phase diagrams of more complicated systems (with five or more components) have not been considered